

Influence of deviation of section angle of attack in serially produced hydrofoils on the lift-drag characteristics

MARINE 2023

Zbigniew Macikowski^{1*}, Artur Karczewski¹ and Przemysław Krata¹

¹ Gdańsk University of Technology, ul. Gabriela Narutowicza 11/12, 80-233 Gdańsk, Poland

* Corresponding author: Zbigniew Macikowski, zbigniew.macikowski@pg.edu.pl

ABSTRACT

Hydrofoils are designed to achieve specified characteristics, but in most cases, the final product is not an ideal design representation. In the case of sailing racing, where hydrofoils are made of composite materials, competitors notice vast differences in the performance of the same products. Differences in performance are significant even within products produced by one manufacturer in one production series. This article addresses the problem of assessing the influence of deviation of the angle of attack on lift-drag characteristics for serially produced hydrofoils.

In total, ten hydrofoils were measured. They were produced by one manufacturer for the monotype racing class and are made of carbon fiber composite. The first measurement was done by 3D scanning, and obtained models were analysed in Rhino3D. The parameters of foils and their sections were measured using codes written in the Grasshopper plugin. From a practical point of view, 3D scanning was too time-consuming and expensive to measure a larger number of foils. Therefore, the alternative method for measuring hydrofoil geometry was proposed. Physical measurement was introduced, which allowed testing more foils but was limited to measuring specified parameters. Parameters were chosen arbitrarily and had to be possible to measure on existing foils. During the experiment following quantities were measured: foil span, foil tip coordinates, angle of attack for specified sections, sections' coordinates (for specified locations defined by foil mounting holes), and sections' chord lengths.

The aim of this article is to show the influence of differences in angles of attack for corresponding sections of hydrofoils on lift and drag characteristics. We began by comparing the foils' geometry. The first criterion for comparison was the symmetry of both sides of the hydrofoil. Secondly, differences between foils for the same section were compared. Next, ranges and typical deviations of the angle of attack for this population were defined.

Characteristics of wings were calculated by performing CFD simulations using OpenFOAM. The finite volume method with steady, turbulent k-w SST flow models was applied. Calculations were performed for scanned hydrofoils and models with a modified angle of attack at particular sections based on previously defined ranges. The calculations allowed defining the influence of changes in the angle of attack on foil lift and drag for the specified magnitude of deviations.

Keywords: Drag, hydrodynamics, hydrofoils, lift

NOMENCLATURE

C_L	Hydrodynamic force coefficient in the x -direction [-]
C_D	Hydrodynamic force coefficient in the z -direction [-]
AoA	Angle of attack
CFD	Computational Fluid Dynamics

1. INTRODUCTION

Vessels utilizing hydrofoils have been known for a long time but with an introduction to America's Cup, they became gaining popularity in sailing. They were also introduced in smaller water crafts such as small monohulls, catamarans, windsurfing, and kitesurfing. It quickly became standard for modern racing classes to use hydrofoils. They were also included in Olympic Games by converting Nacra 17 class, introducing Kitesurfing, and replacing the RS:X windsurfing class with the new IQ Foil.

To give equal winning chances most classes have some kind of limitations determining each competitor has the same equipment hence the same chance to win from the technical point of view. Moreover, in Olympic classes competitors are limited to purchasing equipment from specified licensed manufacturers, and modifications for foils are restricted to slight sanding (The IKA Formula Kite Class Rules 2023, International IQFOIL Class Rules 2022, Nacra 17 Class Rules 2023).

Hydrofoils are designed to achieve specified characteristics, but in most cases, the final product is not an ideal design representation. In the case of sailing crafts racing, where hydrofoils are made of composite materials, competitors noticed vast differences in the performance of the same products. Those differences were as reported significant even within products produced by one manufacturer in one production series. For professional sailors, this means they have to test multiple parts to select the "best" available for them. The scientific perspective lead us to undertake the quantitative assessment of how the hydrofoils' performance is affected or improved by the recorded realistic variations in the resultant geometry that vary from the designed one.

Considering changes in hydrofoil geometry mostly is mentioned in the context of fluid-structure interaction where geometry is changed by forces introduced on it. An experimental investigation of the influence of such changes on foil performance was presented by Zarruk (2014). Another approach for changing the hydrofoil shape is presented by Sacher (2018) by adding flexible elements to the hydrofoil. All of these approaches are based on ideal design geometry. In the case of using existing hydrofoil as base investigation interesting work is presented by Knudsen (2023) using scans of Nacra 17 as the base for geometry used later for velocity prediction. But none of these approaches considers changes in a hydrofoil geometry which are the outcome of the production process.

In this paper, we focus only on existing, post-production geometry accounting for the geometry imperfections, excluding the design process. This paper aims to investigate differences in sections' angles of attack in produced hydrofoils and examine the influence of deviations on foil performance.

2. METHODS AND MATERIALS

For this paper, 10 hydrofoils were 3D scanned and the angles of attack for each wing were measured. Using scanned geometry "idealized" 3D model was prepared to represent the desired set of changes in geometry. Next CFD simulations were carried out to investigate changes in hydrofoils' performance.

2.1 Hydrofoil geometry

All scanned foils were produced by one manufacturer and according to their approval for the racing class, should have the same geometry. The manufacturer does not publish specific hydrofoil design parameters except for a wing span of 900 mm. This dimension also includes the fuselage which is 30 mm wide and this gives 435 mm of actual foil span for each side. A special stand was constructed to capture differences in geometry. It allowed the positioning of hydrofoils in relation to the mounting point during the scanning process. This means that we measure differences as if foil was mounted on the craft. The scanning process was carried out by an outside company so the exact scanning parameters are unknown.

2.2 Measurements of hydrofoil geometric parameters

Section curves and data were obtained using an algorithm written in Rhino Grasshopper. For each hydrofoil following quantities were measured: foil span, foil tip coordinates, angle of attack for specified sections, sections' coordinates (for specified locations defined by foil mounting holes), and sections' chord lengths. As for the sections' angle of attack, they were defined by measuring the vertical location (in the plane of the section) for the leading and trailing edges. And then knowing the section's length the angle of attack was calculated. All measurements shown in this paper were made on 3D scans.

2.3 Defining idealized model of the wing

As scanned foils' geometry differs vastly and has a number of global and local deviations for the purpose of CFD calculations “an idealized” model of geometry was proposed. The model was built using Rhino with the Grasshopper plugin. It was build basing on one of the scanned foils. In this model, sections were smoothed to remove local imperfections, and the trailing edge was rebuilt to be more suitable for later meshing. Locations of sections were kept as they were for the existing wing. As a baseline, each section in the model has an angle of attack of 0 degrees and is later rotated to the desired value. Next surface geometry is built on the sections. The final surface of the model is shown in Figure 1.

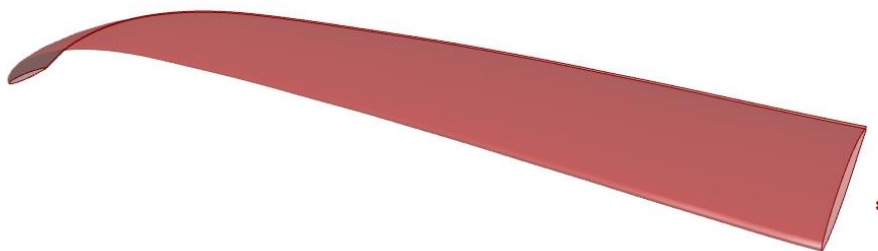


Figure 1. View of idealized model geometry.

Table 1. Idealized model main dimensions.

Wing span	0.435 m
Wing area	0.04 m ²
Avg. section length	0.092 m

2.4 CFD simulation

CFD simulations were carried out using OpenFOAM (version 2206) software. As angles of attack in all cases are small, a steady-state solver was chosen (simpleFOAM). For Turbulence modeling k-Omega SST model was used.

The first step of preparation was an investigation into the influence of mesh refinement on results. For this purpose series of simulations were conducted for refinement levels from 7 to 10 (base mesh cell size is divided by 2 to the power of refinement level) with a mesh of base cell size of 0.32 mm. Simulations were carried out for NACA 0009 hydrofoil, this geometry also later was used for validation purposes.

Validation of CFD simulation was done by comparing the results of CFD simulation with the experimental results presented by Zarruk (2014). Hydrofoil in this experiment has similar sizes to the later examined wing, and they operate for similar Reynold's number. For validation, lift and drag coefficients for 5 angles of attack were compared with ones from an experiment.

For mesh used during experiment refinement level 9 was chosen (cell size 0.000625 mm) with additional refinement for regions near edges (cell size 0.0003215 mm). A total of 9 inflation layers was added on the geometry surface with a target minimal thickness of the first layer equal to 0.00001 mm. All mesh parameters are presented in Table 2.

Table 2. Mesh cell sizes and dimensions.

	Size [m]	Refinement level	Cell size [mm]
Domain	2.88 x 1.92 x 1.28	0	0.32
Field refinement	1.6 x 0.96 x 1.28	2	0.08
Refinement box 1	1.42 x 0.64 x 0.48	4	0.02
Refinement box 2	0.8 x 0.54 x 0.24	6	0.005
Refinement box 3	0.28 x 0.45 x 0.09*	7	0.0025
Wing surface		9	0.000625
		10	0.0003215
First inflation layer			0.00001

3. RESULTS

3.1 Results of measurement of the angle of attack of considered wings

Firstly results of scan measurements are presented. They are later used as a baseline for CFD simulations. In Figure 2 are shown angles of attack for measured sections for each scanned foil. Position of section is measured from hydrofoil mounting point in directions of wing tips this means that for example section with position of 100 mm should correspond to section with position of -100 mm.

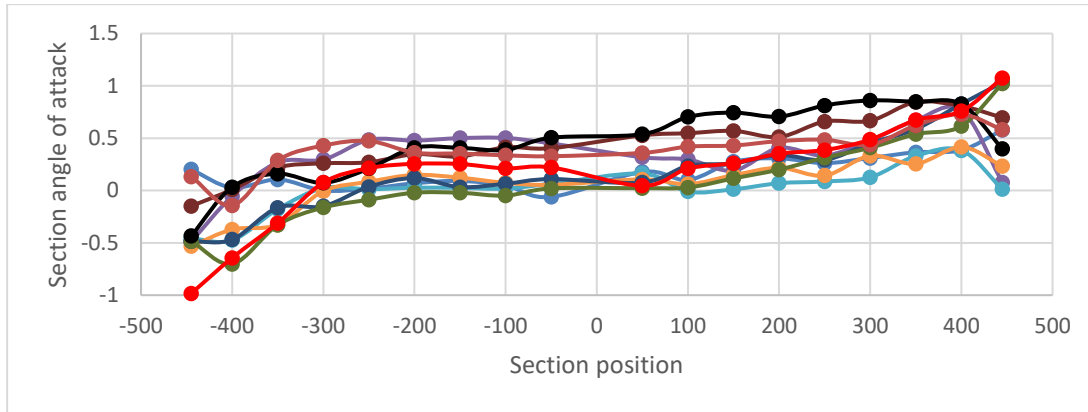


Figure 2. Sections' angles of attack for measured wings.

For each hydrofoil difference in the angle of attack of corresponding sections is calculated. The average values of differences are presented in Table 4.

Table 4. Average values of differences in angle of attack for corresponding sections.

Section position [mm]	50	100	150	200	250	300	350	400	450
Average AoA difference [deg]	0.092	0.108	0.156	0.153	0.236	0.372	0.600	0.930	0.939

Assuming that in the designed hydrofoil each side is identical we treated each side as a separate foil for later calculations. Values of average angle and extreme values for each set of sections are presented in table 5.

Table 5. Minimum, maximum, average value and range of values of angles of attack of section.

Location of section [mm]	50	100	150	200	250	300	350	400	445
Min. AoA [deg]	-0.061	-0.048	-0.022	-0.021	-0.088	-0.162	-0.330	-0.702	-0.984
Max. AoA [deg]	0.538	0.702	0.745	0.707	0.812	0.861	0.847	0.827	1.075
Avg. AoA [deg]	0.221	0.230	0.255	0.289	0.274	0.270	0.273	0.186	0.101
AoA range [deg]	0.599	0.751	0.766	0.728	0.900	1.023	1.177	1.529	2.059

Measurements of the angle of attack for sections closest to the fuselage revealed a spread of about 0.6 degrees for the measured population of wings. For tip sections, this value is almost twice as high. For

some wings changes in the angle of attack have fluid progression but in many cases, changes are not fluid and foil has some odd sections. The average angle of attack for particular sections is between 0.1 to 0.3 degrees. Angles of sections located near the fuselage are mostly between values of 0 to 0.5 degree and from 200 mm from the middle of the hydrofoil the range start to spread significantly.

In the model linear progression of the angle of attack was assumed. The first section 3 values were chosen (0; 0.25; 0,5 [deg]) for the wingtip section 6 values were chosen (-0.5; -0.25; 0; 0.25; 0,5; 0.75 [deg]).

3.2 CFD validation results

Firstly mesh size study is presented, followed by the comparison of CFD results with the experiment for NACA 0009. Figure 3 displays the results of how the drag coefficient is affected by mesh refinement level.

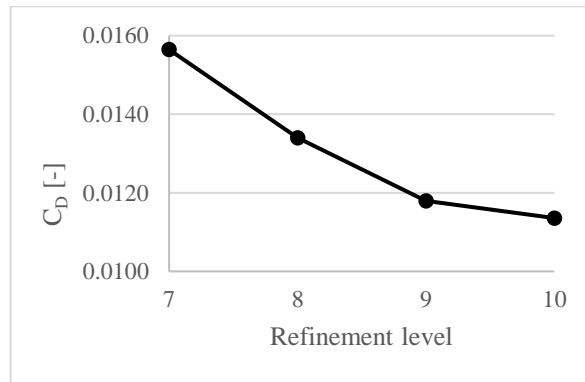


Figure 3. Change of drag coefficient with change mesh refinement level.

For lift coefficient values of the simulation are almost identical to the ones from an experiment (represented in Figure 4).

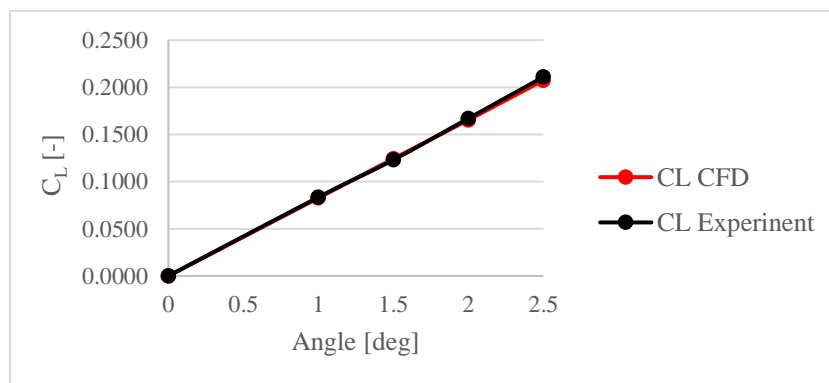


Figure 4. Comparison of experimental data and CFD calculations for lift coefficient for NACA 0009 profile.

For Drag coefficient calculated values are higher but the error for different angles of attack is constant (represented in Figure 5). As the values of coefficients for CFD simulations were close to the experimental ones and the error for drag coefficient is constant for shown range, we assume that the model is sufficient for calculating differences between hydrofoils.

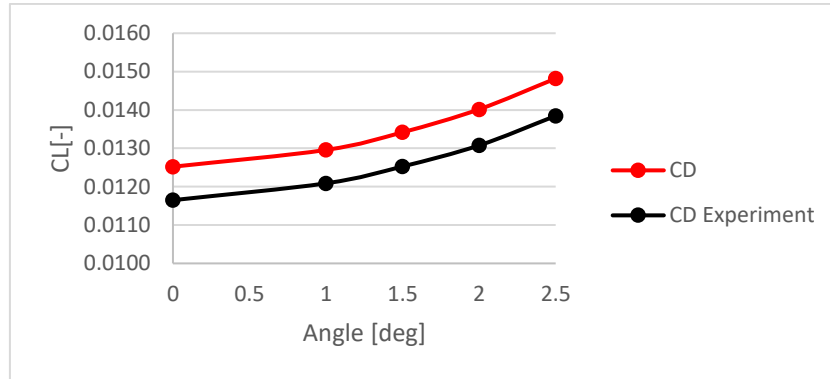


Figure 5. Comparison of experimental data and CFD calculations for drag coefficient for NACA 0009 profile.

3.3 Result of CFD simulations

A total of 18 simulations were carried out. For each case, a different angle of attack for the first and last sections was chosen. The case angle of attack and naming is shown in Table 6. The base case was case number 3 for which all the sections have the angle of attack equal to 0 degrees.

Table 5. Angle of attacks for cases and case naming.

		last section angle of attack [deg]					
		-0.5	-0.25	0	0.25	0.5	0.75
first section angle of attack [deg]	0	1	2	3	4	5	6
	0.25	7	8	9	10	11	12
	0.5	13	14	15	16	17	18

As a result of simulations lift and drag were calculated and are presented in the form of drag and lift coefficients in Figure 6, where, for the sake of clarity of presentation, the test points are named according to the scheme presented in Table 5. In the figures, three sets of results are presented each set corresponding to a different angle of attack in the first section. Values are presented for different values of angles of attack in the last section.

For both lift and drag coefficient values are growing with the increase of angle of attack. For lift coefficient difference between the lowest and highest value in the measured range is 0.07. The highest value in the range is 49% higher than the base case and the lowest is 11% lower. Lift coefficient values are shown in Figure 6.

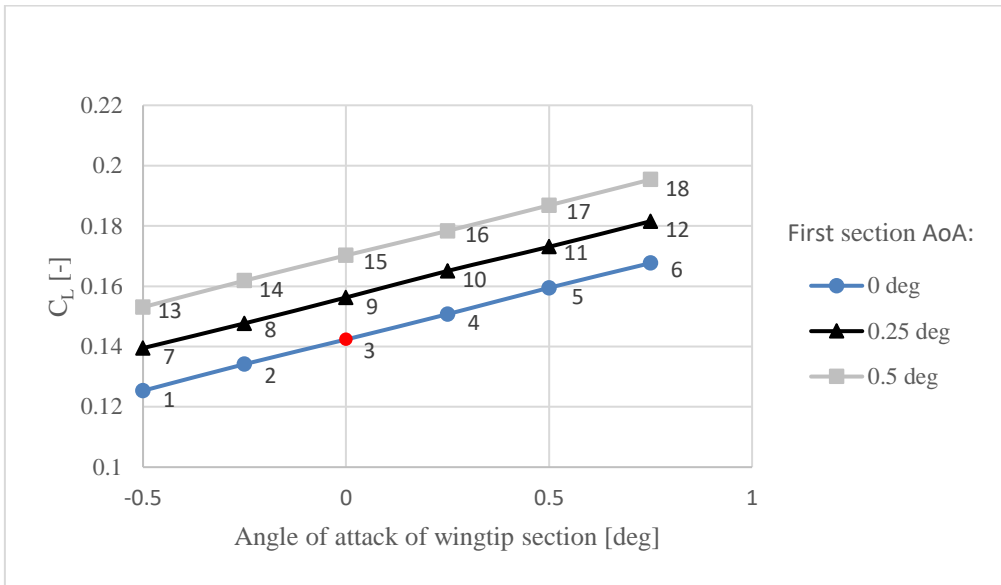


Figure 6. Values of lift coefficient for different angles of attack configurations.

For drag coefficient changes are lower with a 5% increase from baseline for the highest drag and a 0.6% decrease for the lowest drag value. Results for the drag coefficient are presented in Figure 7.

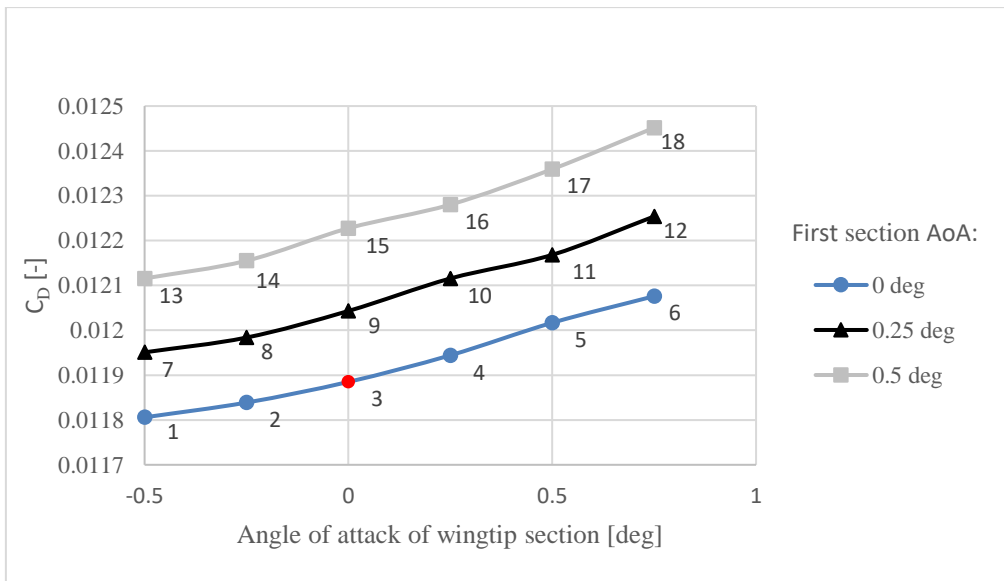


Figure 7. Values of drag coefficient for different angles of attack configurations.

In Figure 8 lift-to-drag ratio is the present value. As differences in the lift are much higher than in drag lift to drag ratio is increasing with the increase of angles of attack in the measured range.

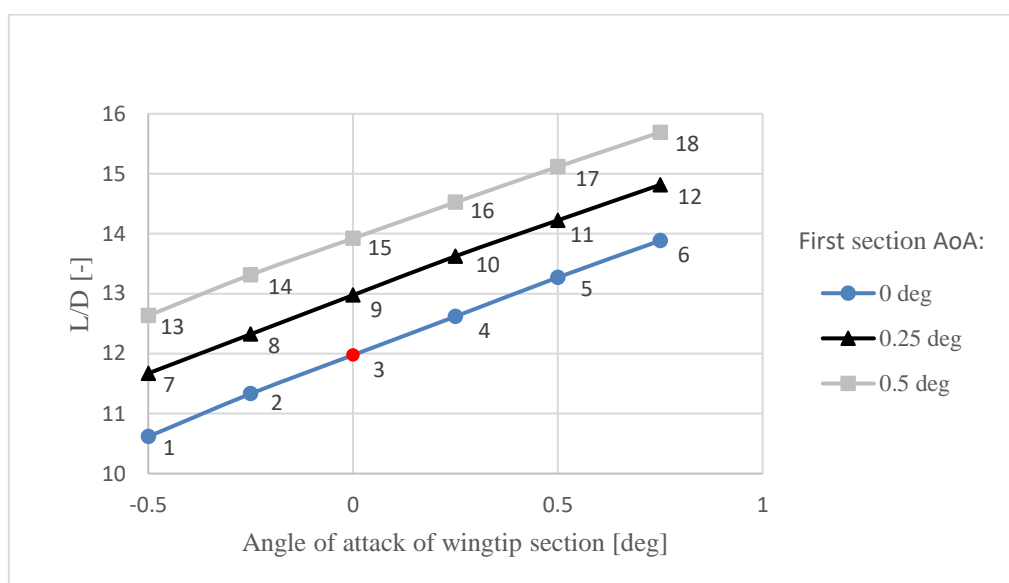


Figure 7. Values of lift to drag ratio for different angles of attack configurations.

4. DISCUSSION

The results of measurements have revealed significant differences in the hydrofoils' angle of attack. CFD simulations show the major impact of these differences on wing lift and drag. When designing new equipment, we can adjust the angle of attack of the foil to optimize its performance. However, for existing equipment, it may not always be possible to adjust the angle of attack without affecting the position of other submerged parts and the rig. Given the range of observed differences, it is reasonable to conduct further research on this matter.

To build an accurate model of the hydrofoil, this study used 3D scans for measurements. However, using this method for a larger number of scans would be too expensive and time-consuming. To address this issue, the contact method was introduced to measure specific traits of the wing. This approach will be used in future research to include more hydrofoils in the study.

Measured wings differ from each other in many ways. This makes results of research focused exclusively on the angle of attack impossible to relate to existing pieces of equipment. This motivates us to extend this research by adding other parameters of a wing into consideration.

5. CONCLUSION

The research aimed to investigate the influence of deviations in the angle of attack for serially produced hydrofoils. For 10 hydrofoils angles of attack were defined based on 3D scanned geometry and for 18 configurations lift and drag were calculated using CFD simulation. The results show that production differences in angle of attack have a major impact on wing characteristics. This correlate with observations made by sailors. Future work would consider the influence of the remaining geometrical parameters of the hydrofoil and increase the sample size of measured wings.

REFERENCES

- Knudsen, S. S., Walther, J. H., Legarth, B. N., & Shao, Y. (2023). Towards Dynamic Velocity Prediction of NACRA 17. *Journal of Sailing Technology*, 8(1), 1–23. <http://onepetro.org/JST/article-pdf/8/01/1/3065319/sname-jst-2023-01.pdf/1>
- Sacher, M., Durand, M., Berrini, É., Hauville, F., Duvigneau, R., le Maître, O., & Astolfi, J. A. (2018). Flexible hydrofoil optimization for the 35th America's Cup with constrained EGO method. *Ocean Engineering*, 157, 62–72. <https://doi.org/10.1016/J.OCEANENG.2018.03.047>
- Garg, N., Pearce, B. W., Brandner, P. A., Phillips, A. W., Martins, J. R. R. A., & Young, Y. L. (2019). Experimental investigation of a hydrofoil designed via hydrostructural optimization. *Journal of Fluids and Structures*, 84, 243–262. <https://doi.org/10.1016/J.JFLUIDSTRUCTS.2018.10.010>
- Sacher, M., Durand, M., Berrini, É., Hauville, F., Duvigneau, R., le Maître, O., & Astolfi, J. A. (2018). Flexible hydrofoil optimization for the 35th America's Cup with constrained EGO method. *Ocean Engineering*, 157, 62–72. <https://doi.org/10.1016/J.OCEANENG.2018.03.047>
- Zarruk, G. A., Brandner, P. A., Pearce, B. W., & Phillips, A. W. (2014). Experimental study of the steady fluid-structure interaction of flexible hydrofoils. *Journal of Fluids and Structures*, 51, 326–343. <https://doi.org/10.1016/j.jfluidstructs.2014.09.009>
- The IKA Formula Kite Class rules 2023-02-06, Sailing.org
- International IQFOIL Class Rules 2022-04-01, Sailing.org
- Nacra 17 Class Rules 28th 02(Feb) 2023, Sailing.org